

A governing relationship for repetitive muscular contraction

J.C. Martin^{a,*}, N.A. Brown^b, F.C. Anderson^b, W.W. Spirduso^b

^aDepartment of Exercise Science, School of Public Health, The University of South Carolina, 1300 Wheat St., Columbia, SC, 29208, USA

^bThe University of Texas at Austin, USA

Accepted 3 February 2000

Abstract

During repetitive contractions, muscular work has been shown to exhibit complex relationships with muscle strain length, cycle frequency, and muscle shortening velocity. Those complex relationships make it difficult to predict muscular performance for any specific set of movement parameters. We hypothesized that the relationship of impulse with cyclic velocity (the product of shortening velocity and cycle frequency) would be independent of strain length and that impulse–cyclic velocity relationships for maximal cycling would be similar to those of in situ muscle performing repetitive contraction. Impulse and power were measured during maximal cycle ergometry with five cycle-crank lengths (120–220 mm). Kinematic data were recorded to determine the relationship of pedal speed with joint angular velocity. Previously reported in situ data for rat plantaris were used to calculate values for impulse and cyclic velocity. Kinematic data indicated that pedal speed was highly correlated with joint angular velocity at the hip, knee, and ankle and was, therefore, considered a valid indicator of muscle shortening velocity. Cycling impulse–cyclic velocity relationships for each crank length were closely approximated by a rectangular hyperbola. Data for all crank lengths were also closely approximated by a single hyperbola, however, impulse produced on the 120 mm cranks differed significantly from that on all other cranks. In situ impulse–cyclic velocity relationships exhibited similar characteristics to those of cycling. The convergence of the impulse–cyclic velocity relationships from most crank and strain lengths suggests that impulse–cyclic velocity represents a governing relationship for repetitive muscular contraction and thus a single equation can predict muscle performance for a wide range of functional activities. The similarity of characteristics exhibited by cycling and in situ muscle suggests that cycling can serve as a window through which to observe basic muscle function and that investigators can examine similar questions with in vivo and in situ models. © 2000 Elsevier Science Ltd. All rights reserved.

Keywords: Force; Work; Power; Cycling; Muscle mechanics

1. Introduction

The contractile properties of skeletal muscle are well understood. Force–velocity, force–length, and force–excitation properties have been determined via a reductionist approach in which one property is varied while all others are held constant. Those properties, however, may not represent muscle function during in vivo activities. Rather, many voluntary movements require that the muscle become activated, produce force while shortening, relax, and undergo lengthening before contracting again. Thus, it is useful to understand not just the isolated contractile properties, but also how these properties function in concert with one another.

Muscle function during repetitive contraction has been investigated using the work-loop technique (Josephson, 1985) in which in situ muscle is cyclically shortened and lengthened, and stimulated to contract for a portion of the cycle. Investigators who have used this technique have reported complex relationships between muscular work and movement parameters. To date, no governing relationship relating muscle function to the movement parameters has been reported.

The main factors that affect muscle force are length, shortening velocity, and excitation state. Although muscle length affects force during static contraction, this effect is greatly reduced following stretch (Edman et al., 1978) and thus force is relatively independent of length during repetitive contractions. The product of cycle frequency and length change (strain) determines average shortening velocity and thus affects muscle force via force–velocity characteristics. Cycle frequency also

* Corresponding author. + 1-803-777-6887; fax: + 1-803-777-8422.
E-mail address: jcmartin@sph.sc.edu (J.C. Martin).

affects muscle force via excitation state. Specifically, incomplete excitation associated with activation and relaxation kinetics reduces force output, compared with the force produced by a muscle in the fully excited state. These kinetics, especially relaxation kinetics, have been shown to exert increasingly greater effect at higher frequency (Caiozzo and Baldwin, 1997). During repetitive contractions, then, cycle frequency may serve as an indicator of the average excitation state. Further, the product of muscle shortening velocity and cycle frequency (“cyclic velocity”) should provide a more thorough description of a muscle’s capacity to produce force than either shortening velocity or cycle frequency alone. Finally, because the variables that affect repetitive contraction are time dependent, it may be appropriate to use a time-dependent measure, such as mechanical impulse (force integrated over time), to describe muscular function.

The purpose of the present investigation was to test the hypotheses that impulse–cyclic velocity relationships would be independent of strain length and that maximal cycling impulse–cyclic velocity relationships would be similar to those of in situ muscle performing repetitive contraction. Cycling exercise was used because the legs are constrained to cyclically flex and extend by the cranks, and therefore, each mono-articular muscle must undergo cyclic length changes similar to those imposed during work loops. These hypotheses, if confirmed, would reveal a governing relationship for repetitive muscle contraction and allow a priori prediction of muscular performance for a wide range of functional activities for in vivo and in situ models.

2. Methods

Our hypotheses were tested in three phases: (1) kinematic data were recorded and analyzed to determine if pedal speed was a valid predictor of joint angular velocity, (2) impulse and power were measured during maximal cycling on five cycle-crank lengths and across a range of pedaling frequencies, and (3) data previously reported by Swoap et al. (1997) for in situ repetitive contraction were used to calculate values for impulse, shortening velocity, and cyclic velocity.

Fifteen male cyclists (age: 28 ± 6 yr, height: 179 ± 6 cm, mass: 74 ± 7 kg; mean \pm SD) volunteered to participate in this investigation. The procedures were explained and the subjects provided written informed consent. This investigation was approved by the Institutional Review Board at The University of Texas at Austin.

Maximal cycling was performed on crank lengths of 120, 145, 170, 195, and 220 mm. Familiarization trials were performed on all crank lengths during the week prior to data collection. On each experimental data collection day, subjects performed a 5-min warm-up of

steady-state cycling at 100 W and four maximal cycling bouts on one crank length. Crank lengths were presented in a randomized counterbalanced design with four ordering sequences. During a separate protocol, kinematic data were obtained during steady-state cycling.

The relationships of pedal speed with joint angular velocity at the hip, knee, and ankle were determined for pedaling frequencies of 0.42, 0.83, 1.25, 1.67, 2.08, and 2.50 Hz on all five crank lengths during steady-state cycling. These data were obtained for three of the original 15 subjects who represented the shortest, median, and longest leg length. Reflective markers were placed at the greater trochanter, lateral femoral condyle, lateral malleolus, lateral calcaneus, and at the head of the fifth metatarsal. Trajectories of reflective markers were recorded using a three-camera kinematic data collection system and a frame rate of 60 Hz. The three-dimensional coordinates of all markers in each frame were digitized. Position data were filtered using a fourth-order Butterworth filter with a cutoff frequency of 6 Hz. Joint angular velocities were calculated from position data using finite differentiation. Averaged values of joint angular velocity for the leg extension phase (crank angle of 0–180°) were calculated for six consecutive revolutions within each trial.

Maximal cycling impulse and power were measured using the inertial load method (Martin et al., 1997) which determines torque delivered to an ergometer flywheel across a range of pedaling frequencies. The ergometer was fitted with bicycle-racing handlebars, cranks, pedals, and seat, and was fixed to the floor. Each subject wore cycling shoes fitted with a cleat that locked into a spring-loaded binding on the pedal.

A slotted disc was mounted on the flywheel and an infra-red photodiode and detector were mounted on the ergometer frame on opposite sides of the disc. The slots were spaced at $\pi/8$ rad ($\Delta\theta$) along the perimeter of the disc and they alternately passed or interrupted the infra-red light beam. The detector circuit emitted a square pulse at each interrupt. The time between consecutive interrupts (Δt) was recorded by a dedicated microprocessor with a clock accuracy of ± 500 ps. Flywheel angular velocity was calculated as $\Delta\theta/\Delta t$. The time–angular velocity data were low-pass filtered at 8 Hz and angular acceleration was determined as the first time derivative of the time–velocity data using a fifth-order spline (Woltring, 1986). Incremental values for torque, force, impulse, and power were calculated for each measured data point. Flywheel torque was calculated as the product of angular acceleration and flywheel moment of inertia with no frictional resistance applied to the flywheel. Crank torque was calculated as the product of flywheel torque and gear ratio. Pedal force was calculated as crank torque divided by crank length (i.e. net force normal to the crank). Impulse was calculated as the product of pedal force and Δt . Power was calculated as the product of flywheel

moment of inertia, angular velocity, and angular acceleration.

The incremental values for impulse and power were used to calculate values for each complete cycle (i.e. the reported values) beginning with either leg. Impulse for each cycle was calculated as the sum of the incremental impulse values. Power for each cycle was calculated as the mean of the incremental power values. Pedaling frequency was the reciprocal of the time for each cycle. Pedal speed was calculated from pedaling frequency and crank length ($2\pi f \times \text{crank length}$). Cyclic velocity was defined as the product of pedal speed and cycle frequency.

This method has been described previously (Martin et al., 1997). In the present investigation, changes were made to the original protocol, including the length of the crank, the inertial load, and the number of crank revolutions. The inertial load was varied (e.g. 6.5 kg m² for the 120 mm cranks; 12.1 kg m² for the 220 mm cranks) by adjusting the gear ratio (Martin et al., 1997) so that the inertial resistance at the pedal was similar for all crank lengths. The number of crank revolutions in each test was varied to match total work across all the crank lengths (e.g. 6.5 revolutions for the 220 mm cranks; 9.0 revolutions for the 120 mm cranks). This approach allowed the subjects to reach optimal pedaling frequency within approximately 2–3 s, and to complete the test in approximately 3–4 s. Seat height was set to match each subject's accustomed riding position and was adjusted so that the maximum distance from the top of the saddle to the pedal axle (in its most extended position) was constant for all crank lengths.

Mechanical work (W), cycle frequency (f), and strain length (L) reported by Swoap et al. (1997) for in situ rat plantaris muscle were used to estimate mechanical impulse and shortening velocity. Impulse was calculated as work divided by the product of cycle frequency and strain length ($I = W/(f \times L)$). Mean shortening velocity was calculated from cycle frequency and strain length ($V_s = 2 \times f \times L$). In situ cyclic velocity was defined as the product of mean shortening velocity and cycle frequency.

Linear regression was used to determine the relationship of pedal speed with joint angular velocity at the hip, knee, and ankle. A rectangular hyperbola ($\text{Impulse} = b(I_0 + a)/(V_{\text{cyc}} + b) - a$, where I_0 is the maximum impulse, and a and b are constants with units of impulse and cyclic velocity, respectively) was fitted to the cycling impulse–cyclic velocity data for each crank length using non-linear regression. To determine if impulse–cyclic velocity relationships were truly independent of crank length, impulse values were determined by linear interpolation for cyclic velocity values of 3–8 Hz m/s for each bout and analyzed with a repeated measures analysis of variance. If a significant main effect for crank length was detected, a Bonferonni post hoc procedure was used to determine which crank lengths differed.

A rectangular hyperbola was fitted to the in situ impulse–cyclic velocity data for each strain length using non-linear regression. A single rectangular hyperbola was fitted to the impulse–cyclic velocity data from all strain lengths and to data from strains 2–7 mm.

3. Results

Pedal speed was highly related to joint-angular velocities at the hip, knee, and ankle (Fig. 1) and therefore serves as a valid marker for muscle shortening velocity. The regression equations were:

$$\omega_{\text{Hip}} = 1.22 \times \text{PS} + 0.10 \quad R^2 = 0.97 \quad p < 0.001$$

$$\text{SEE} = 0.016 \text{ rad/s (1\%)},$$

$$\omega_{\text{Knee}} = 2.00 \times \text{PS} + 0.22 \quad R^2 = 0.96 \quad p < 0.001$$

$$\text{SEE} = 0.029 \text{ rad/s (0.6\%)},$$

$$\omega_{\text{Ankle}} = 0.61 \times \text{PS} + 0.19 \quad R^2 = 0.78 \quad p < 0.001$$

$$\text{SEE} = 0.021 \text{ rad/s (2.7\%)}.$$

The cycling impulse–cyclic velocity relationships from the various crank lengths tended to converge onto a single curve, however, the relationship for the 120 mm cranks differed from those of the other crank lengths. The impulse–frequency relationships for each crank length were curvilinear and stratified such that, for any specific frequency, impulse was greater on the shorter crank (Fig. 2A). The impulse–pedal speed relationships for each crank length were also curvilinear, but the order of stratification was reversed (Fig. 2B). For any specific pedal speed, impulse was greater for the longer crank. The impulse–cyclic velocity relationships for each crank length (Fig. 2C) were closely approximated by a rectangular hyperbola ($R^2 = 0.997 \pm 0.000\text{SD}$). A single rectangular hyperbola also provided an excellent approximation to the impulse–cyclic velocity data from all five crank lengths for each subject

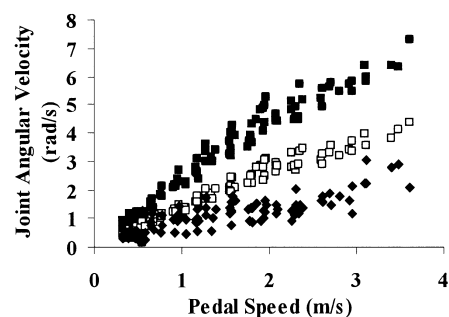


Fig. 1. Pedal speed vs. joint angular velocity. Across five crank lengths and a six-fold range in pedaling rates, PS accounted for 97% of the variation in hip joint angular velocity (\square), 96% of the variation in knee joint angular velocity (\blacksquare) and 78% of the variation on ankle joint angular velocity (\blacklozenge).

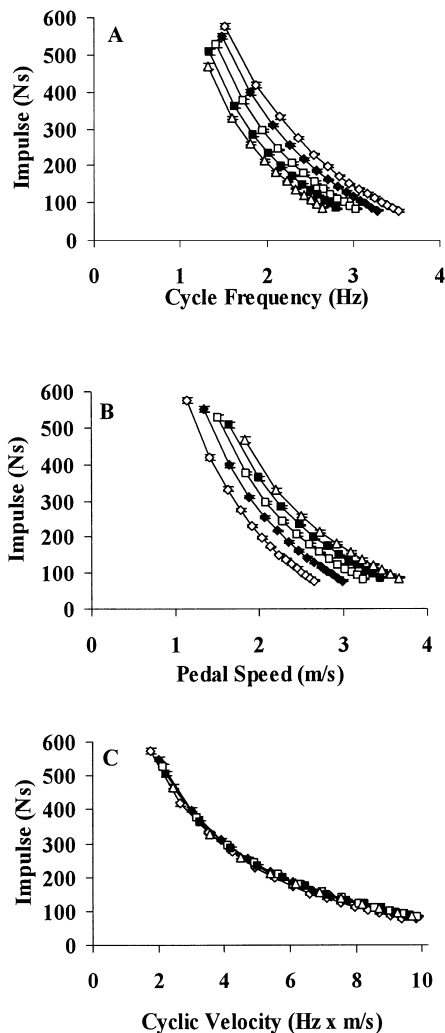


Fig. 2. Mean (\pm SE, $N = 15$) cycling impulse for five crank lengths (\diamond 120 mm, \blacklozenge 145 mm, \square 170 mm, \blacksquare 195 mm, and \triangle 220 mm). Impulse is plotted against cycle frequency (A), pedal speed (B), and cyclic velocity (C). The cycling impulse–cyclic velocity relationships for each crank length were well described by a rectangular hyperbola ($R^2 > 0.99$). Although the effects of crank length were small, impulse for the 120 mm cranks differed significantly from that for all other cranks.

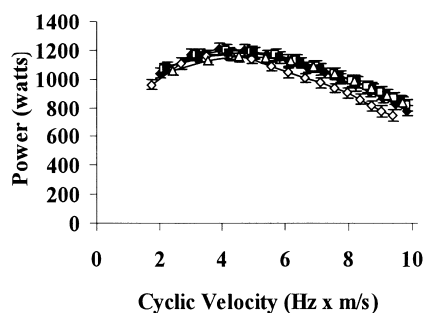


Fig. 3. Mean (\pm SE, $N = 15$) cycling power for five crank lengths (\diamond 120 mm, \blacklozenge 145 mm, \square 170 mm, \blacksquare 195 mm, and \triangle 220 mm).

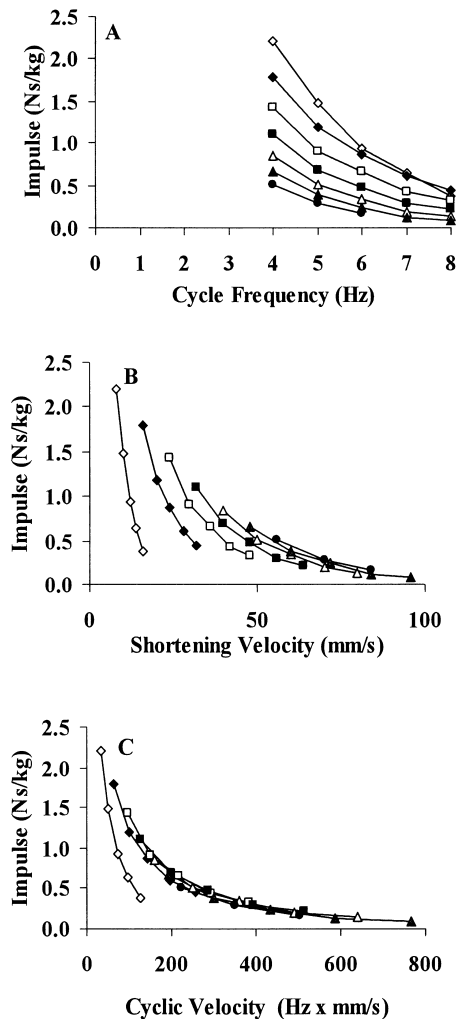


Fig. 4. In situ impulse for seven strain lengths (\diamond 1 mm, \blacklozenge 2 mm, \square 3 mm, \blacksquare 4 mm, \triangle 5 mm, \blacktriangle 6 mm, and \bullet 7 mm). Impulse is plotted against cycle frequency (A), shortening velocity (B), and cyclic velocity (C). The in situ impulse–cyclic velocity relationships for each strain length were well described by a rectangular hyperbola ($R^2 > 0.99$).

($R^2 = 0.997 \pm 0.000SD$). Despite the apparent convergence of the impulse–cyclic velocity relationships, analysis of variance and the Bonferonni post hoc procedure revealed that the relationship for the 120 mm cranks differed from those for all other crank lengths (Fig. 2C).

Relationships calculated for in situ muscle preparation were characteristically similar to those of those produced during human cycling. The impulse–frequency relationships for each strain length were curvilinear, and were stratified such that, for any specific frequency, impulse was greater for the shorter strain (Fig. 4A). The impulse–shortening velocity relationships for each strain length were also curvilinear, but the order of stratification was reversed (Fig. 4B). For any specific shortening velocity, impulse was greater for the longer strain. The impulse–cyclic velocity relationships for each strain length (Fig. 4C) were well described by a rectangular

hyperbola ($R^2 = 0.995 \pm 0.008\text{SD}$) and the stratification was greatly reduced. The impulse–cyclic velocity relationship for all strain lengths was well described by a single rectangular hyperbola ($R^2 > 0.87$). The impulse–cyclic velocity relationship for strain lengths 2–7 mm was even more closely described by a single rectangular hyperbola ($R^2 > 0.987$).

4. Discussion

The main findings of this investigation were: (1) the impulse–cyclic velocity relationships from maximal cycling and in situ work-loops were independent of crank or strain length except for the shortest lengths, and (2) impulse–cyclic velocity relationships were similar for cycling and for in situ muscle contraction. These results suggest that the impulse–cyclic velocity relationship represents a governing relationship for repetitive muscular contraction over a wide range of cycle frequencies and ranges of motion (or strain lengths) except for very small movements. The fact that the impulse–cyclic velocity curves exhibited the same characteristic shape as the traditional force–velocity curve suggests that the impulse–cyclic velocity relationship represents muscle force–velocity characteristics, excitation state, and the measurement interval.

Maximal human cycling produced similar impulse–frequency, impulse–pedal speed (shortening velocity) and impulse–cyclic velocity relationships to those of in situ muscle. This similarity occurred because mechanical energy is almost completely conserved when cycling at high work rates (Broker and Gregor, 1994). Therefore, impulse delivered to the skeletal system is almost completely transferred to the cycle cranks. Even though the present data are from cycling, they have implications for more general actions because in situ work loops have been shown to be predictive of locomotor activity in animals (Hammond et al., 1998; Johnson et al., 1994; Marsh, 1990; Wakeling and Johnston, 1998).

Although impulse–cyclic velocity relationships for most strain and crank lengths converged onto one curve, data for the 120 mm cranks differed from all other cranks and in situ data for the 1 mm strain clearly differs from those of the other strain lengths (Figs. 2C and 4C). These differences are probably related to tendon compliance. Specifically, at small strain, tendon compliance may allow the contractile unit to shorten at a higher velocity than that of the muscle–tendon unit. Consequently, impulse may be reduced due to force–velocity characteristics. However, the impulse–cyclic velocity relationships for crank lengths greater than 120 mm did not differ, and a single rectangular hyperbola accounted for 98.7% of the variation in impulse for strain lengths of 2–7 mm. Thus, above some threshold strain, the effects of tendon compliance are reduced and the impulse–cyclic velocity

relationship is independent of strain. These results suggest that impulse–cyclic velocity governs the behavior of the contractile unit but may not always govern the behavior of the muscle–tendon unit.

Muscle shortening velocity cannot be directly determined during cycling, however, our kinematic data showed that pedal speed was highly related to joint angular velocity. This was a key relationship because the length of muscles that extend the hip and knee have been reported to be highly correlated with joint angle of the hip and knee (Visser et al., 1990; Hawkins and Hull, 1990). It follows that joint angular velocity and muscle shortening velocity should also be highly related. Pedal speed, therefore, provides a valid indication of muscle shortening velocity.

Impulse–frequency relationships (Figs. 2A and 4A) were stratified because, for any specific cycle frequency, longer crank or strain lengths elicit greater shortening velocities. Thus, impulse was reduced due to force–velocity characteristics. Conversely, impulse–pedal speed (or shortening velocity) relationships (Figs. 2B and 4B) were stratified because shorter cranks must rotate at higher frequency to achieve any specific pedal speed. Thus, impulse was reduced due to decreased excitation and shorter time interval. While muscle force–velocity characteristics are well known (Hill, 1938), the effects of cycle frequency on muscle excitation have only recently been demonstrated. Caiozzo and Baldwin (1997) reported that force was reduced during activation and relaxation, and that the time required for activation and relaxation occupied a larger portion of the cycle at higher frequencies. Consequently, average excitation was reduced with increasing frequency. Cyclic velocity represents the shortening velocity and average excitation state, and impulse accounts for the measurement interval. Thus, those variables represent the main factors that govern muscular contraction.

Mechanical impulse was used to quantify muscular performance because it is a function of cycle time and muscular force. An equally compelling reason to consider impulse is that the impulse–cyclic velocity and power–cyclic velocity relations are analogous to the traditional force–velocity and power–velocity relations. Specifically, both force \times velocity (N m/s) and impulse \times cyclic velocity (N s Hz m/s) have units of power. Power is equal to impulse \times cyclic velocity only if force is constant throughout the cycle, which it is not. However, a regression analysis of our cycling data revealed that the product of impulse and cyclic velocity was highly correlated with and approximately equal to power ($R^2 > 0.98$). Indeed, if the axes of Figs. 2C and 3 were not labeled, they might be easily mistaken for traditional force– and power–velocity relationships. Thus, conceptually and practically, impulse– and power–cyclic velocity relations are analogous to the traditional force– and power–velocity relations.

The impulse–cyclic velocity relationships seemed to be unaffected by muscle force–length properties. This might seem surprising, because each cycle–crank length elicited a different range of motion and an in situ strain length of 7 mm (10% greater than resting length for the rat plantaris) should reduce isometric force by approximately 7% (Woittiez et al., 1984). However, Edman et al. (1978) reported that force was nearly constant from resting length to 25% above resting length following stretch. Thus, the length independence of the impulse–cyclic velocity relationships is probably due to stretch enhanced force production.

Cycling data were presented in linear coordinates even though they were calculated from angular data. All the relationships reported for cycling impulse can also be shown in angular coordinates: angular impulse–cyclic velocity, where angular impulse is the integral of torque over the time for one cycle and cyclic velocity is the product of angular velocity and cycle frequency. This is true because our value of pedal force represents only force directed normal to the crank. If a pedal dynamometer were used to measure orthogonal pedaling forces, linear and angular impulse would differ somewhat. However, the index of effectiveness (ratio of normal-to-total force applied to the cranks) has been reported to be 63–69% for trained cyclists (Coyle et al., 1991), suggesting that most pedal force is directed normal to the crank. Additionally, Broker and Gregor (1996) reported that most forces exerted tangent to the crank are of gravitational and inertial origin. Thus, the muscular portion of linear and angular impulse is quite similar. Linear coordinates were used to simplify comparison with in situ data.

In summary, these data demonstrated that impulse–cyclic velocity relationships were independent of strain or crank length above some threshold length. Thus, a single equation describes and can predict muscle performance for a wide range of functional activities. Additionally, muscle characteristics during cycling were similar to those observed in situ, suggesting that cycling serves as a window through which to observe basic muscle function and that investigators can examine similar questions with in vivo and in situ models.

Acknowledgements

The authors would like to extend their sincere gratitude to the subjects who volunteered and enthusiastically participated in this investigation. We would also like to thank those who have provided advice, critique, and debate during the preparation of this manuscript: Doug-

las A. Syme, Andrew R. Coggan, Roger P. Farrar, Walter Herzog, Richard R. Neptune, Jeffery P. Broker, and E. Donald Stevens.

References

- Broker, J.P., Gregor, R.J., 1994. Mechanical energy management in cycling: source relations and energy expenditure. *Medicine and Science in Sports and Exercise* 26, 64–74.
- Broker, J.P., Gregor, R.J., 1996. Cycling biomechanics: fundamental pedaling dynamics and force “ineffectiveness”. In: Burke, E. (Ed.), *High-Tech Cycling*. Human Kinetics, Champaign, IL, pp. 152–154.
- Caiozzo, V.J., Baldwin, K.M., 1997. Determinants of work produced by skeletal muscle: potential limitations of activation and relaxation. *American Journal of Physiology* 273, C1049–1056.
- Coyle, E.F., Feltner, M.E., Kautz, S.A., Hamilton, M.T., Montain, S.J., Baylor, A.M., Abraham, L.D., Petrek, G.W., 1991. Physiological and biomechanical factors associated with elite endurance cycling performance. *Medicine and Science in Sports and Exercise* 23, 93–107.
- Edman, K.A., Elzinga, G., Noble, M.I., 1978. Enhancement of mechanical performance by stretch during tetanic contractions of vertebrate skeletal muscle fibres. *Journal of Physiology (London)* 281, 139–155.
- Hammond, L., Altringham, J.D., Wardle, C.S., 1998. Myotomal slow muscle function of rainbow trout *Oncorhynchus mykiss* during steady swimming. *Journal of Experimental Biology* 201, 1659–1671.
- Hawkins, D., Hull, M.L., 1990. A method for determining lower extremity muscle-tendon lengths during flexion/extension movements. *Journal of Biomechanics* 23, 487–494.
- Hill, A.V., 1938. The heat of shortening and dynamic constants of muscle. *Proceedings of Royal Society of London B* 126, 136–195.
- Johnson, T.P., Syme, D.A., Jayne, B.C., Lauder, G.V., Bennett, A.F., 1994. Modeling red muscle power output during steady and unsteady swimming in largemouth bass. *American Journal of Physiology* 267, R481–488.
- Josephson, R.K., 1985. Mechanical power output from striated muscle during cyclic contraction. *Journal of Experimental Biology* 114, 493–512.
- Marsh, R.L., 1990. Deactivation rate and shortening velocity as determinants of contractile frequency. *American Journal of Physiology* 259, R223–230.
- Martin, J.C., Wagner, B.M., Coyle, E.F., 1997. Inertial-load method determines maximal cycling power in a single exercise bout. *Medicine and Science in Sports and Exercise* 29, 1505–1512.
- Swoap, S.J., Caiozzo, V.J., Baldwin, K.M., 1997. Optimal shortening velocities for in situ power production of rat soleus and plantaris muscles. *American Journal of Physiology* 273, C1057–1063.
- Visser, J.J., Hoogkamer, J.E., Bobbert, M.F., Huijing, P.A., 1990. Length and moment arm of human leg muscles as a function of knee and hip-joint angles. *European Journal of Applied Physiology* 61, 453–460.
- Wakeling, J.M., Johnston, I.A., 1998. Muscle power output limits fast-start performance in fish. *Journal of Physiology (London)* 201, 1505–1526.
- Woittiez, R.D., Huijing, P.A., Boom, H.B., Rozendal, R.H., 1984. A three-dimensional muscle model: a quantified relation between form and function of skeletal muscles. *Journal of Morphology* 182, 95–113.
- Woltring, H.J., 1986. A FORTRAN package for generalized, cross-validatory spline smoothing and differentiation. *Advances in Engineering Software* 8, 104–113.